Journal of Inflammation Research

Dovepress
Taylor & Francis Group

Open Access Full Text Article

ORIGINAL RESEARCH

Single-Nucleus and Bulk RNA Sequencing Reveals the Involvement of Natural Killer and CD8$^+$ T Cells in the Progression of Androgenetic Alopecia

Haijing Fu[1], Wumei Zhao[1], Leiwei Jiang[2,3], Shijun Shan[1,4]

[1]Department of Dermatology, Xiang'an Hospital of Xiamen University, School of Medicine, Xiamen University, Xiamen, 361000, People's Republic of China; [2]Department of Dermatology, Guizhou Provincial People's Hospital, Guiyang City, Guizhou Province, People's Republic of China; [3]GuiYang First People Hospital, Guiyang, 550002, People's Republic of China; [4]College of Mathematical Medicine, Zhejiang Normal University, Jinhua, 321004, People's Republic of China

Correspondence: Shijun Shan; Leiwei Jiang, Email shanshijun2023@163.com; leiweijiang@163.com.Abstract

Background: Androgenetic alopecia (AGA) is the most common type of androgen-associated hair loss. Emerging evidence highlights inflammation as a critical mediator in follicular miniaturization and disease progression. This investigation systematically explores inflammatory mechanisms in AGA through comprehensive analysis of hair follicles transcriptional profiles combined with cellular heterogeneity.

Methods: Matched follicular specimens were procured from AGA patients: occipital non-balding units (controls) versus frontal alopecic zones (experimental). Bulk RNA-sequencing was conducted on Norwood-Hamilton grade 3–5 AGA scalp tissues to delineate inflammatory signatures. Subsequent single-nucleus RNA sequencing (snRNA-seq) of grade 5 specimens resolved cellular heterogeneity. Immune subsets (NK/CD8$^+$ T cells), vascular endothelia (BECs), keratinocytes, and fibroblasts were transcriptionally characterized. Findings were validated through immunofluorescence cytochemistry (IFC) and reverse transcription quantitative PCR (RT-qPCR).

Results: Bulk RNA-sequencing of AGA hair follicles revealed heightened inflammatory signatures in grade 5 patients compared to grade 3–4 counterparts. To dissect cellular heterogeneity, we systematically investigated the dynamic changes of immune cells in hair follicles of AGA patients using snRNA-seq technology for the first time. The result showed that grade 5 AGA hair follicles, identifying significant enrichment of natural killer (NK) and CD8$^+$ T cells in balding hair follicles. Concurrently, blood endothelial cells (BECs) in balding follicles exhibited downregulation of angiogenesis-related genes. Notably, IL-15—a cytokine critical for NK/CD8$^+$ T cell proliferation—was overexpressed in BECs, keratinocytes, and fibroblasts, suggesting a microenvironmental cue for immune cell expansion.

Conclusion: These findings collectively implicate NK and CD8$^+$ T cell infiltration as drivers of inflammatory exacerbation in AGA. By blocking IL-15 signaling-mediated immune activation may be an innovative therapeutic approach to promote hair regeneration in AGA patients.

Keywords: androgenetic alopecia, natural killer cells, CD8$^+$ T cells, inflammation and snRNA-seq

Introduction

Hair loss is a global challenge that significantly impacts patients, leading to issues such as obsessive-compulsive disorder, interpersonal sensitivity, depression, and anxiety.[1,2] A substantial number of hair loss cases are attributed to androgenetic alopecia (AGA), which is primarily driven by dysregulation in the microenvironment surrounding hair follicles.[3,4] While factors such as androgen, vascular insufficiency and oxidative stress are often mentioned,[5,6] the role of the inflammation has emerged as a critical component in the pathophysiology of AGA. Although AGA is commonly categorized as a non-inflammatory and non-scarring form of alopecia, histological evidence indicates that inflammation is indeed present.[7] Jaworsky et al found that the normal hair follicles lacked hair follicular inflammation, whereas hair loss regions of AGA patients consistently exhibited activated T cell infiltrates around the lower portions of the hair follicular infundibula.[7] Mahé

Received: 12 February 2025
Accepted: 20 May 2025
Published: 30 May 2025

et al introduced the term "microinflammation" in AGA, and this term is increasingly recognized in the hair follicles of individuals with alopecia. Inflammatory response can lead to progressive fibrosis of the perifollicular sheath, disrupting normal hair cycling and ultimately contributing to hair loss.[8] The presence of inflammation in the hair follicles is emerging as a significant aspect of understanding the complex etiologies of AGA.[9]

It has been established that the immune microenvironment in AGA has significant changes, while the precise patterns of these changes remain unclear. Studies show that the rise in γδ T cells, central memory $CD8^+$ T cells, activated $CD8^+$ T cells, and the infiltration of mast cells have contributed to changes in the immune microenvironment in AGA.[10] Hair follicle stem cells (HFSCs) are crucial for the coordinated regeneration of hair follicles. Perifollicular T lymphocytes serve as critical modulators of HFSCs state transitions—encompassing quiescence, proliferation, and differentiation—across homeostatic and pathophysiological conditions.[11] Disruption of this dynamic relationship can lead to significant hair loss. An imbalance in immune cell infiltration may affect the hair follicle cycles, contributing to hair loss.[12] However, research on immune infiltration in male AGA is limited.

The hair follicle is a miniature organ containing several cellular components. Due to the intricate cellular composition of the hair follicle, the depth of single-cell RNA sequencing is constrained, making it challenging to accurately detect specific components like the cortex, medulla, and matrix.[13] To further explore the role of different cell in AGA, we utilized bulk RNA-seq and snRNA-seq to analyze the immune differences between the forehead alopecia area (balding group) and the normal occipital region (control group) in AGA patients.

Method

Selection of Human Samples

Human hair follicle samples were obtained from patients with AGA who underwent hair transplant surgery. This study was approved by the Human Research Ethics Committee of Xiang'an Hospital of Xiamen University (XAHLL2023011) and adhered to the principles outlined in the Declaration of Helsinki. Prior to their participation, written informed consent was obtained from all individuals involved. Exclusion criteria included: use of hair growth-promoting agents (eg, finasteride, minoxidil) within the past 18 months; use of immunomodulatory medications (eg, corticosteroids, immunosuppressants) or participation in other drug trials within the past 3 months; and presence of severe visceral/cutaneous diseases affecting hair growth or any systemic disorders. All samples were obtained from AGA patients, with the control group consisting of hair follicles harvested from the non-balding occipital region and the experimental group comprising follicles collected from the frontal balding area. RNA-seq analysis was performed on hair follicles from 9 AGA patients (three patients in each of Hamilton grades 3 to 5), and snRNA-seq was conducted on hair follicles from 3 grade 5 AGA patients, all aged 25–40 years. The detailed information of the study participants is provided in Supplementary Data 1.

Bulk RNA Sequencing

RNA was extracted from frozen hair follicles using Trizol (Alkali Scientific, TRZ-100). The differences in transcript abundance between different genotypes were calculated for each gene using the R package DESeq2 (version 1.30.0). Genes with adjusted P-value < 0.05 were considered to be differentially expressed.

Nucleus Isolation, Sequencing, and Cell Clustering

Eligible participants were males aged 25–40 years with grade 5 AGA patients. Hair follicle samples were placed in liquid nitrogen and processed for nucleus isolation, followed by sequencing according to the guidelines of 10X Genomics (USA). The cell-by-gene matrices for each sample were individually imported to Seurat (version 3.1.1)[14] for downstream analysis. To reduce the impact of batch effects and behavioral conditions on clustering, we employed Harmony, an algorithm that maps cells into a common embedding where cells are grouped by cell type rather than dataset-specific factors, allowing us to aggregate all samples. The Harmony algorithm takes a PCA embedding of cells along with their batch assignments as input and produces a batch-corrected embedding as output.[15] For visualization of clusters, uniform manifold approximation and projection (UMAP) and t-distributed Stochastic Neighbor Embedding (t-SNE) was generated.[16]

Differentially Expressed Genes Analysis

Kyoto Encyclopedia of Genes and Genomes(KEGG) is a meticulously curated database resource that integrates diverse biological entities categorized into systems, genomic information, chemical data, and health-related information.[17] Differentially expressed genes (DEGs) were analyzed using the KEGG database to identify enriched pathways, with significant terms ($p < 0.05$) highlighted. Additionally, gene expression was assessed through gene set enrichment analysis (GSEA), which revealed hallmark gene sets that were either upregulated or downregulated.

Reverse Transcription-Quantitative Real-time Polymerase Chain Reaction (RT-qPCR) Assay

Total RNA was extracted using NcmZol Reagent (NCM Biotech, China), and cDNA was synthesized using HiScript III Reverse Transcriptase (Vazyme, China). ChamQ Universal SYBR qPCR master mix (Vazyme, China) was used for the RT-qPCR. The primers used are shown in Table 1.

Immunofluorescence

Human hair follicle samples were fixed in 10% neutral buffered formalin for 24 h and dehydrated using the LEICA ASP 200S tissue processor. Then processed for paraffin embedding and blocks were sectioned at 10uM. Sections were incubated at 60 °C for 1 hour, then subjected to a series of alcohol dips to clean and rehydrate them. Antigen retrieval was performed using a citrate-based solution at 100 °C for 10 minutes, followed by fixation in 4% paraformaldehyde and washing with PBS. The sections were blocked, incubated with primary antibodies overnight at 4 °C, and then with secondary antibodies before imaging with a Leica Aperio Versa 200. Antibodies used included anti-Ki67 (Abcam, ab15580), anti-CD8 (Abcam, ab316778) and anti-CD56 (CST, 3576).

Statistical Analysis

The data are expressed as the mean ± SD from a minimum of three independent biological replicates. Differences between groups were compared using a multiple *t*-test where applicable. A p-value of less than 0.05 was regarded as statistically significant. Statistical analysis was conducted using GraphPad Prism 9.0.

Result

Inflammation in AGA Patients Gradually Intensify as the Progresses

To investigate the cellular and molecular mechanisms about AGA, we conducted bulk RNA sequencing (RNA-seq) and single-nuclei RNA sequencing (snRNA-seq) on samples collected from the forehead alopecia area (balding group) and the normal occipital region (control group) of AGA patients (Figure 1A). Principal component analysis (PCA) demonstrated that

Table 1 Primers Used for RT-qPCR of Genes

Gene	Strand	Primer Sequence
Homo-Tbp	Forward	CCTTGTACCCTTCACCAATGAC
	Reverse	ACAGCCAAGATTCACGGTAGA
Homo- GZMA	Forward	TCTCTCTCAGTTGTCGTTTCTCT
	Reverse	GCAGTCAACACCCAGTCTTTTG
Homo- GZMB	Forward	CCCTGGGAAAACACTCACACA
	Reverse	GCACAACTCAATGGTACTGTCG
Homo- PRF1	Forward	GACTGCCTGACTGTCGAGG
	Reverse	TCCCGGTAGGTTTGGTGGAA
Homo-TNFα	Forward	GAGGCCAAGCCCTGGTATG
	Reverse	CGGGCCGATTGATCTCAGC
Homo- IFNG	Forward	TCGGTAACTGACTTGAATGTCCA
	Reverse	TCGCTTCCCTGTTTTAGCTGC
Homo-CCL5	Forward	CTGCAGAGGATCAAGACAGCA
	Reverse	GCGGGCAATGTAGGCAAAG

https://doi.org/10.2147/JIR.S522458

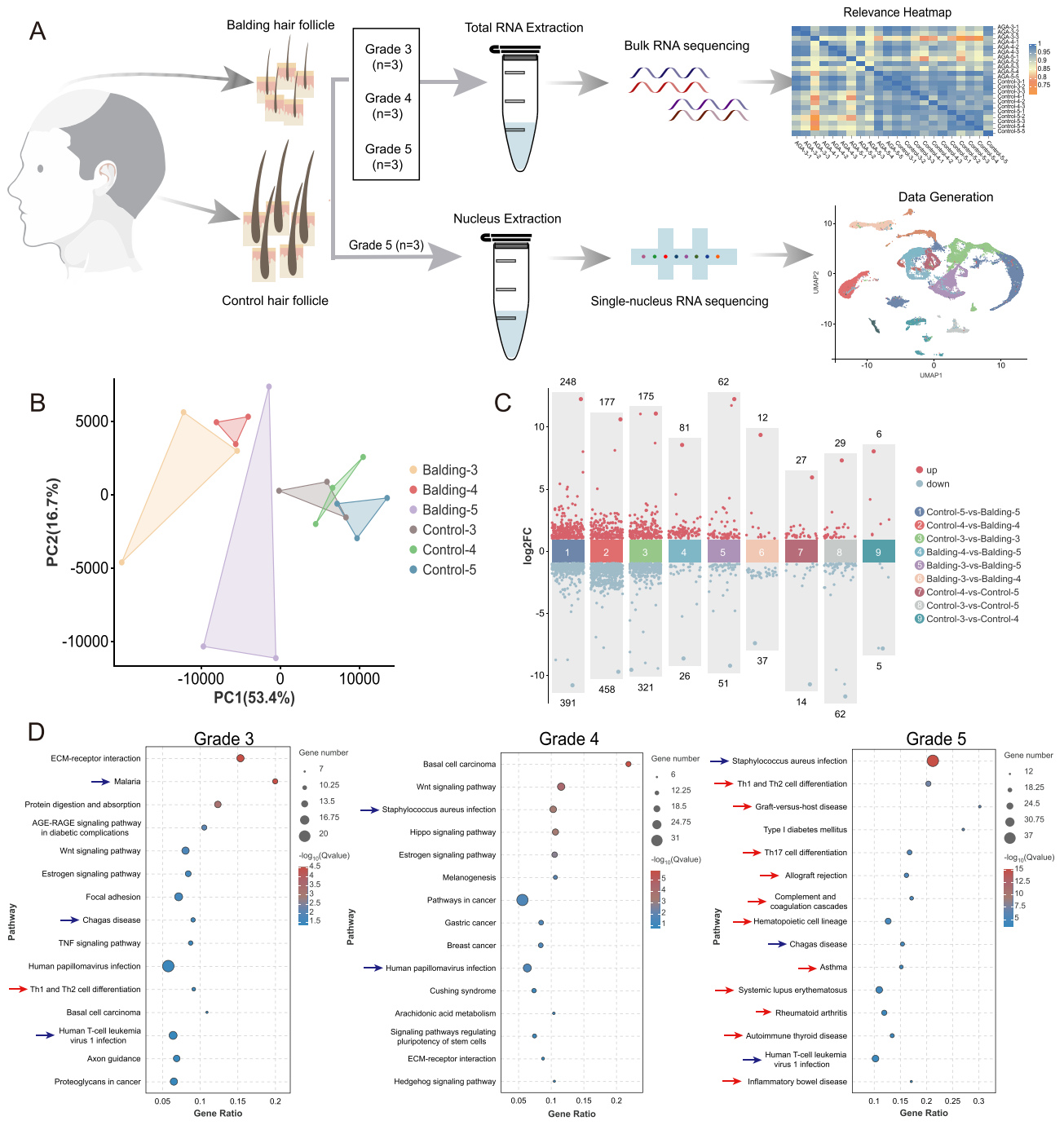

Figure 1 Inflammation in AGA patients gradually intensify as the progresses. (**A**) Flowchart depicting the overall experimental design of this study. The number of patients with bulk RNA sequencing and snRNA-seq were indicated. (**B**) PCA illustrates the clustering of samples from various experimental groups. (**C**) Differential gene expression analysis showing up- and down-regulated genes across all 9 clusters. (**D**) KEGG pathway enrichment analysis of the differentially expressed genes (DEGs) between balding and control group in AGA patients with grades 3–5 (The red arrows indicate immune-related signaling pathways, while the blue arrows indicate pathways associated with bacterial or viral infections).

the transcriptome data were both reliable and reproducible. In patients with AGA grades 3–5, there was little variation in gene expression patterns among the control group, whereas the balding group exhibited distinct gene expression patterns (Figure 1B). We performed differential gene expression (DGE) analysis for each cluster and found that AGA patients with grade 5 had the highest number of differential genes between control and balding samples (Figure 1C). KEGG pathway enrichment analysis of the differentially expressed genes indicated that, among the top 15 enriched signaling pathways, grades

3 and 4 were associated with fewer pathways linked to immune responses and viral or bacterial infections. In contrast, grade 5 has 14 pathways related to immunity and infection (Figure 1D).

snRNA-Seq Map of Hair Follicle Comparing Balding and Control in AGA Patients

Given the pronounced inflammation in grade 5 AGA patients, we selected 3 such patients for snRNA-seq. Their specific hair loss conditions are illustrated in Figure 2A. Control hair follicles were obtained from the normal occipital region, while balding hair follicles were collected from the frontal hair loss area (Figure 2B). Hair follicles were collected from three donors and subjected to snRNA-seq. Multiple markers were then used to separate different cell clusters, resulting in the identification of 15 distinct cell types (Figure 2C, Supplementary Figure 1A and Supplementary Data 2). As expected, the balding samples contained more SG cells and fewer ORS cells than the control hair follicles. Notably, no difference in bulge cells was observed between the balding and the control samples (Supplementary Figure 1B). Identified bulge (*LRIG1*$^+$*SOX9*$^+$ *ITGA6*$^+$),[18–20] ORS (*KRT5*$^+$ *KRT17*$^+$),[21] sebaceous glands (*PPARA*$^+$ *PPARG*$^+$*ELOVL5*$^+$),[22–24] immune (*PTPRC*$^+$),[25] blood endothelial cells (VWF$^+$MCTP1$^+$), fibroblasts (*COL1A1*$^+$*COL3A1*$^+$*DCN*$^+$)[26,27] and keratinocytes (*KRT10*$^+$ *KRT1*$^+$ *S100A8*$^+$)[27] marker genes were cell-type specific and matched the established, traditional markers for each cell population (Figure 2D, Supplementary Figure 1C). In the balding samples, there was a significant lack of proliferating cells, particularly in the matrix, bulge, IRS, and ORS cells (Figure 2E and F).

CD8$^+$ T Cells and NK Cells are the Primary Expanded Immune Population in Balding Hair Follicles

To obtain a detailed profile of immune cells infiltrating the skin, we analyzed immune cell clusters comprising 7515 cells, identifying five lymphoid clusters, three myeloid clusters, and one lymphatic vessel cluster (Figure 3A, Supplementary Figure 2A and Supplementary Data 2). The CD4 clusters included a CD4$^+$ native T-cell cluster with a mix of CD8$^+$ cells (T1: *LEF1*$^+$*IL7R*$^+$*CCR7*$^+$), helper T cells and regulatory T cells (T2: *IL32*$^+$*IL2RA*$^+$*FOXP3*$^+$), and T follicular helper cells (T3: *CXCL13+IL21+ICOS+*) (Figure 3B). We observed a significant cluster of *CD56*$^+$*CD16*$^+$ cells that also contained some CD8$^+$ cells (cluster 0), which we designated as NK_CD8T cells (Figure 3E and Supplementary Figure 2B). Among the transcriptionally distinct subtypes identified, the NK_CD8T cell population was significantly increased in balding compared to control hair follicles (Figure 3C and D, Supplementary Data 3). All NK_CD8T cells expressed the chemokine ligands granzymes A (*GZMA*), natural killer cell granule protein 7 (*NKG7*), and perforin 1 (*PRF1*), which related to cytotoxicity and cell killing[28] (Figure 3E).

The Cytotoxic of CD8$^+$ T and NK Cells Is Increased in the Hair Follicles of AGA Patients with Grade 5

NK cells and CD8$^+$ T lymphocytes can kill target cells by secreting cytokines such as interferon gamma (IFN-γ) and tumor necrosis factor-alpha (TNFα), and by producing cytotoxic granules, including PRF1 and granzymes A, B, K, and M (GZMA, GZMB, GZMK, GZMM).[29,30] To examine the infiltration condition of these immune cells in different grades of AGA, we performed RT-qPCR on hair follicles from the frontal hair loss area and the occipital control region in AGA grade 3, 4, and 5 patients. Our results showed an increase in the expression of *IFNG* and *TNFα* in the frontal hair loss area compared to the occipital control, though this difference was not statistically significant (Figure 4A). Notably, *PRF1* expression was significantly higher in the frontal hair loss area of grade 3–5 AGA patients (Figure 4A). Compared to the control group, the expression levels of *GZMA* and *GZMB* showed an upward trend in balding hair follicles. Furthermore, in grade 5 AGA patients, the expression of *PRF1, GZMA* and *GZMB* were significantly higher in both balding and control hair follicles, compared to grade 3 and grade 4 patients (Figure 4A). Bulk RNA sequencing further revealed significant upregulation of *GZMA, GZMB, GZMM, GZMK, PRF1*, and *NKG7* (Figure 4B). Additionally, *CD27*, which affects NK cell cytotoxicity and cytokine production,[31] was upregulated in balding hair follicles (Figure 4B). We also observed an increase in *CCL5* expression in balding hair follicles; CCL5 is a chemokine primarily produced by NK cells and CD8$^+$ T lymphocytes[32] (Figure 4A and B). Gene set enrichment analysis (GSEA) revealed significant enrichment of natural killer cell mediated cytotoxicity and cytokine-cytokine receptor interaction pathways in the balding group

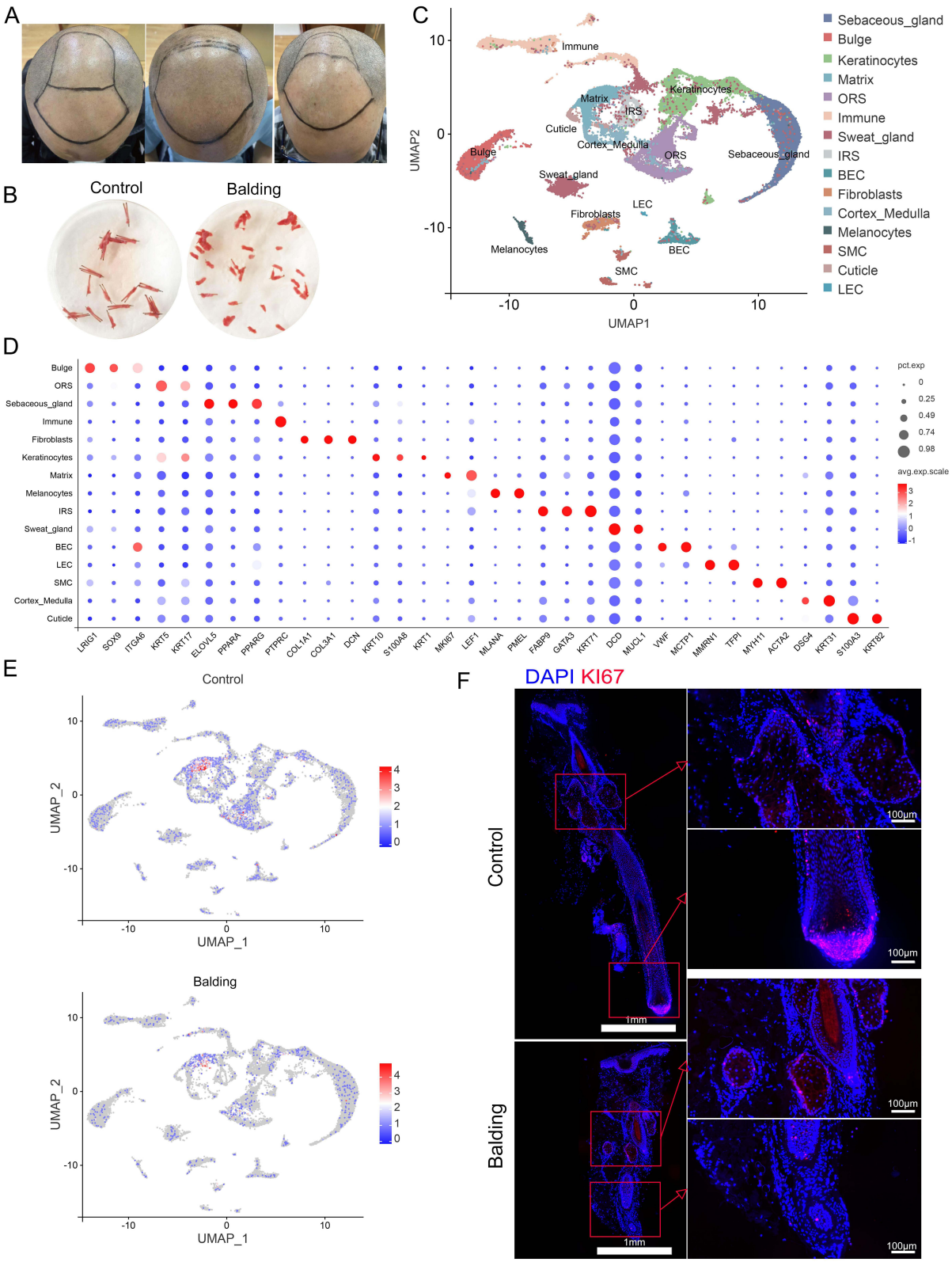

Figure 2 snRNA-seq map of hair follicle comparing balding and control in AGA patients. (**A**) Clinical pictures of the 3 patients that were included in this study with AGA. (**B**) Clinical pictures of control hair follicles from the normal occipital region and balding hair follicles from the frontal hair loss area in AGA patients. (**C**) snRNA-seq of human hair follicle visualized with uniform manifold approximation and projection (UMAP) plot. (**D**) Marker gene expression in 15 cell clusters. (**E**) Feature plots of disease groups showing the proliferation marker *MKI67*. (**F**) Immunostaining of hair follicles with anti-Ki67 (red) and nuclei were counter-stained with 4′,6-diamidino-2-phenylindole (DAPI) (blue). Zoomed-in images are shown in the right panel.

Abbreviations: ORS, outer root sheath; IRS, inner root sheath; BEC, blood endothelial cells; SMC, smooth muscle cells; LEC, lymphatic endothelial cells.

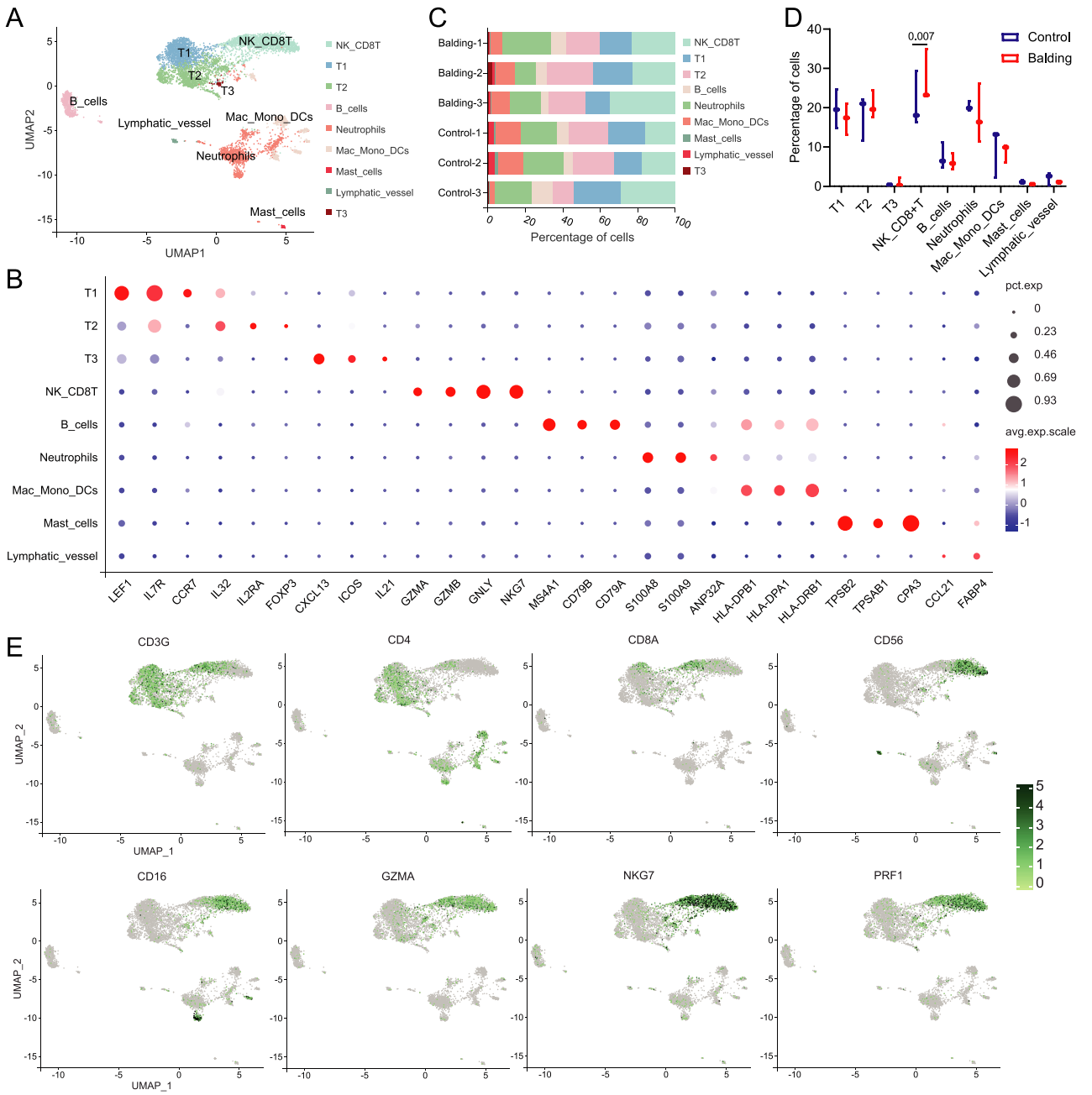

Figure 3 CD8+ T cells and NK cells are the primary expanded immune population in balding hair follicles. (**A**) UMAP plot of the immune cluster. (**B**) Dot plot with canonical markers indicative of respective immune subsets. (**C**) Proportion of cells from major cell types identified in balding and control samples. (**D**) Percentage of each immune cell subset among all immune cells. (**E**) Feature plots of selected NK_CD8T cell canonical genes.
Abbreviations: Mac, Macrophage; Mono, Monocyte; DC, Dendritic cell.

(Figure 4C, Supplementary Figure 2C). Finally, we confirmed the elevated of $CD8^+$ T and $CD56^+$ NK cell at the protein level in balding hair follicles (Figure 4D and E).

The Angiogenic Factors are Reduced in the BECs of Balding Hair Follicles

Next, we examined the effects of NK and $CD8^+$ T cells on other cells within the hair follicle. The results showed that genes related to $CD8^+$ T cell cytotoxicity, such as *RORA*,[33] were upregulated in the BECs, fibroblasts and keratinocytes of balding hair follicles (Figure 5A). Additionally, genes associated with the activation of NK and $CD8^+$ T cells—*IL1R1*,[34] *IL33*[35] and *IL-*

https://doi.org/10.2147/JIR.S522458

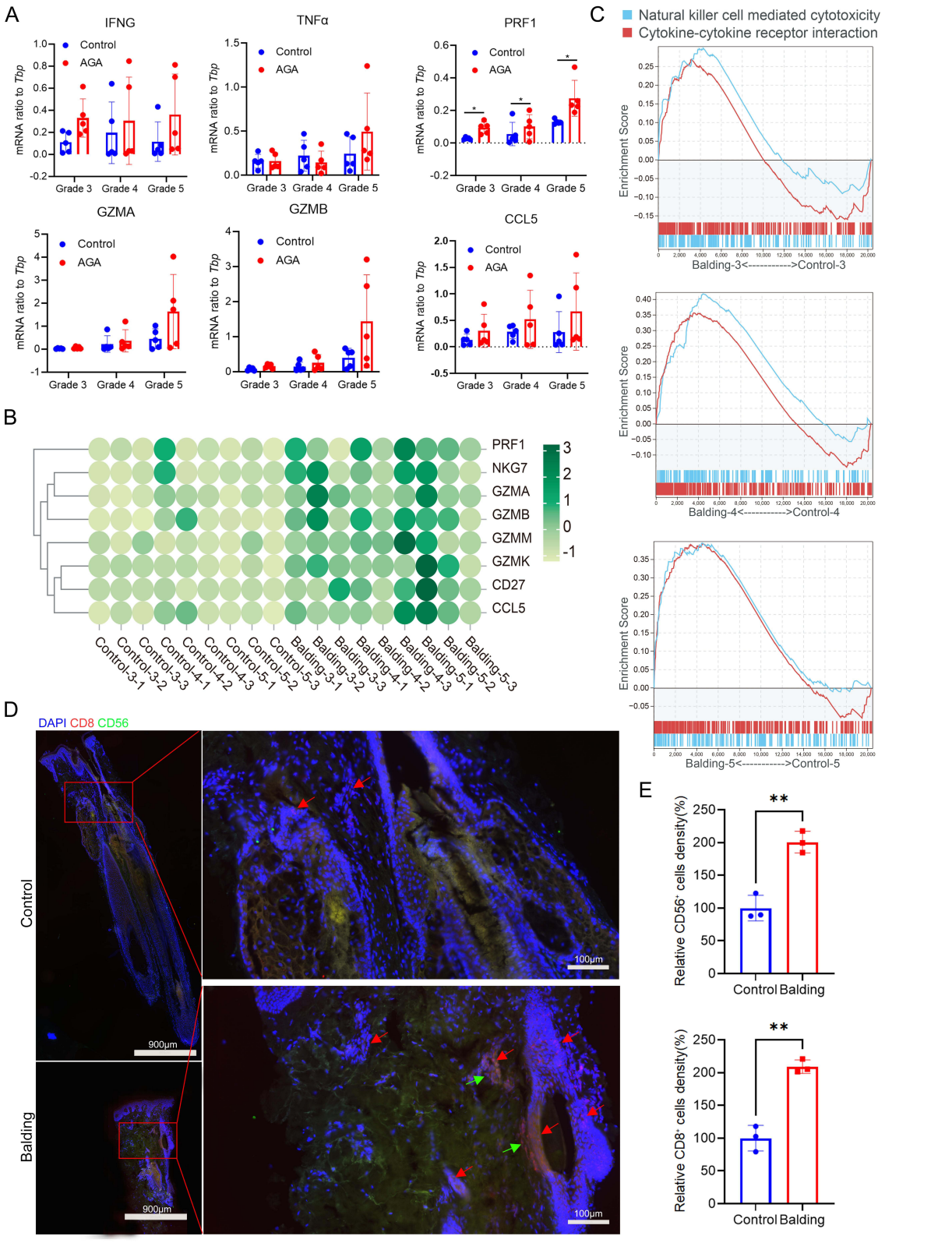

Figure 4 The cytotoxic of CD8$^+$ T and NK cells is increased in the hair follicles of AGA patients with grade 5.(**A**) Measurement of cytotoxicity-associated genes using qRT-PCR (*p < 0.05). (**B**) Heat map illustrating the expression of cytotoxicity-associated genes based on previous profiling studies. (**C**) Gene set enrichment analysis of the natural killer cell-mediated cytotoxicity and cytokine-cytokine receptor interaction pathway in AGA patients with grades 3–5. (**D**) Representative immunofluorescence images showing CD8 and CD56 expression in hair follicles of control and balding. Red arrows indicate CD8-positive cells, green arrows indicate CD56-positive cells. (**E**) Quantification of CD8 and CD56 positive cell in hair follicle (**p < 0.01).

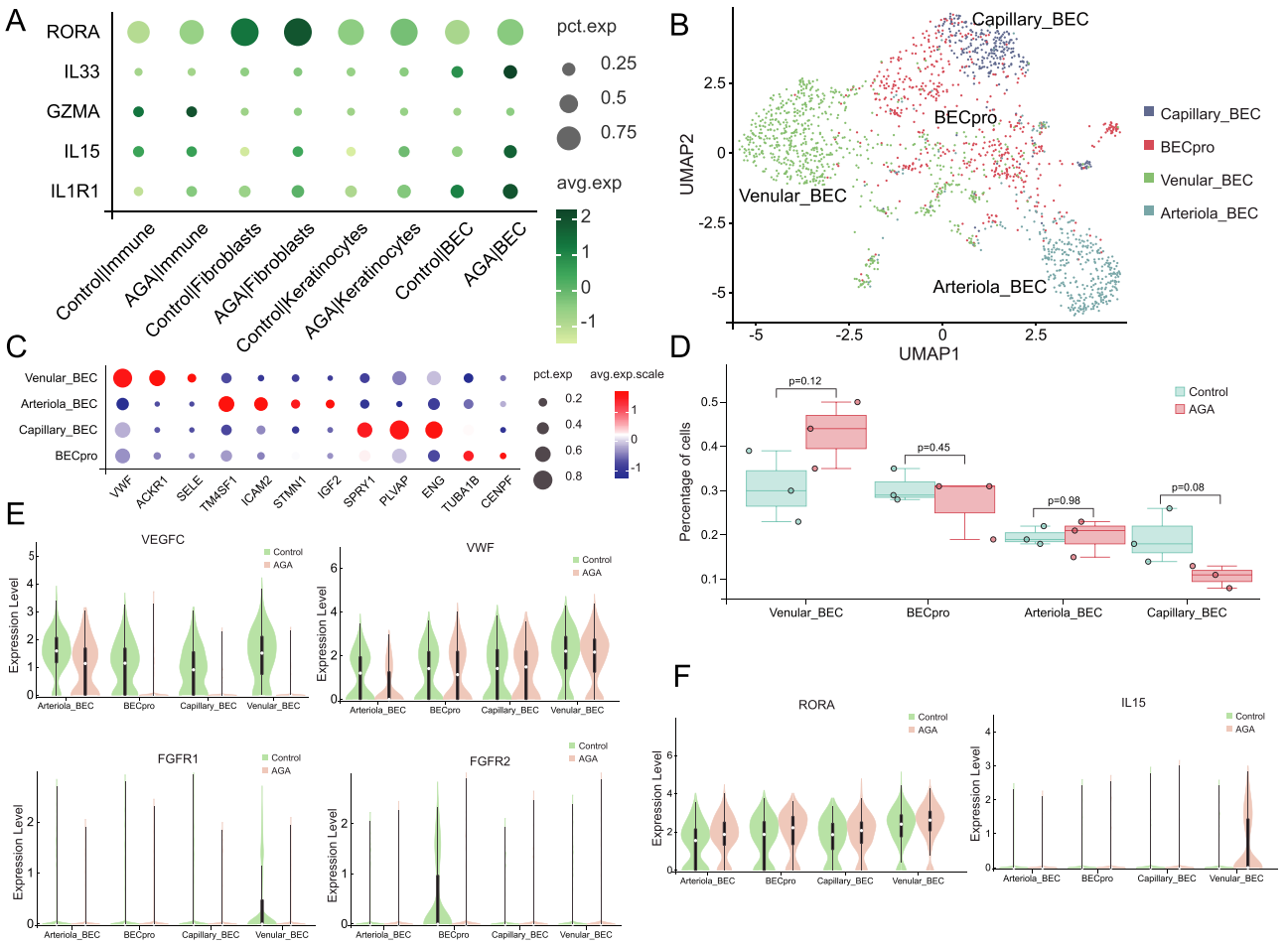

Figure 5 The angiogenic factors are reduced in the BECs of balding hair follicles. (**A**) Dot plot depicting the variations between the control and balding groups for selected genes. (**B**) UMAP visualization representing the BECs cluster. (**C**) Dot plot highlighting canonical markers associated with specific BECs subsets. (**D**) Proportion of each BECs cell subset within the total BECs population. (**E**) Violin plots of selected genes related to angiogenesis. (**F**) Violin plots of NK and CD8+T cell associated genes. Abbr: Blood endothelial cell (BEC); proliferating (pro).

15[36]—were predominantly upregulated in BECs. *IL1R1* and *IL-15* were also upregulated in fibroblasts and keratinocytes. GZMA was upregulated in both immune cells and BECs (Figure 5A).

Within the BECs clusters, we identified four distinct subsets: proliferating BECs (BECpro: *TUBA1B*$^{+}$*CENPF*$^{+}$), venular BECs (*VWF*$^{+}$*ACKR1*$^{+}$*SELE*$^{+}$), arteriolar BECs (*TM4SF1*$^{+}$*ICAM2*$^{+}$*STMN1*$^{+}$*IGF2*$^{+}$), and capillary BECs (*SPRY1*$^{+}$*PLVAP*$^{+}$*ENG*$^{+}$) (Figure 5B and 5C, Supplementary Data 2). The BECs subsets did not show significant differences across the groups (Figure 5D, Supplementary Data 3), but we did observe a decrease in the expression of genes associated with angiogenesis, such as *VEGFC, VWF, FGFR1*, and *FGFR2* (Figure 5E). Interestingly, both *RORA* and *IL15* were elevated in the BECs of balding hair follicles, with *IL15* showing a particularly pronounced increase in venular BECs (Figure 5F).

Compositional Differences in Fibroblasts and Keratinocytes

Among keratinocytes (KCs), subclusters include proliferating KCs (KCpro) marked by *MKI67*$^{+}$*TOP2A*$^{+}$*CENPF*$^{+}$, basal KCs expressing *COL17A1*$^{+}$ *KRT15*$^{+}$ *KRT14*$^{+}$, spinous1 KCs characterized by *KRT6*$^{+}$ *KRT6*$^{+}$ *KRT17*,[+37] spinous2 KCs with *KRT1*$^{+}$ *KRT10*$^{+}$, and supraspinous KCs identified by *SLURP1*$^{+}$ *CALML5*$^{+}$ *SPRR2E*$^{+}$(Figure 6A and B). Additionally, channel cells were found to express "Channel-ATPase" genes (*ATP1A1*$^{+}$ *SAT1*$^{+}$), which regulate ion channels, while eccrine cells were marked by *AQP5*$^{+}$ *KRT19*$^{+}$(Figure 6A and B, Supplementary Data 2). Quantitative analysis revealed no significant differences in the numbers of KCpro, spinous 2, supraspinous, channel, and eccrine cells

https://doi.org/10.2147/JIR.S522458

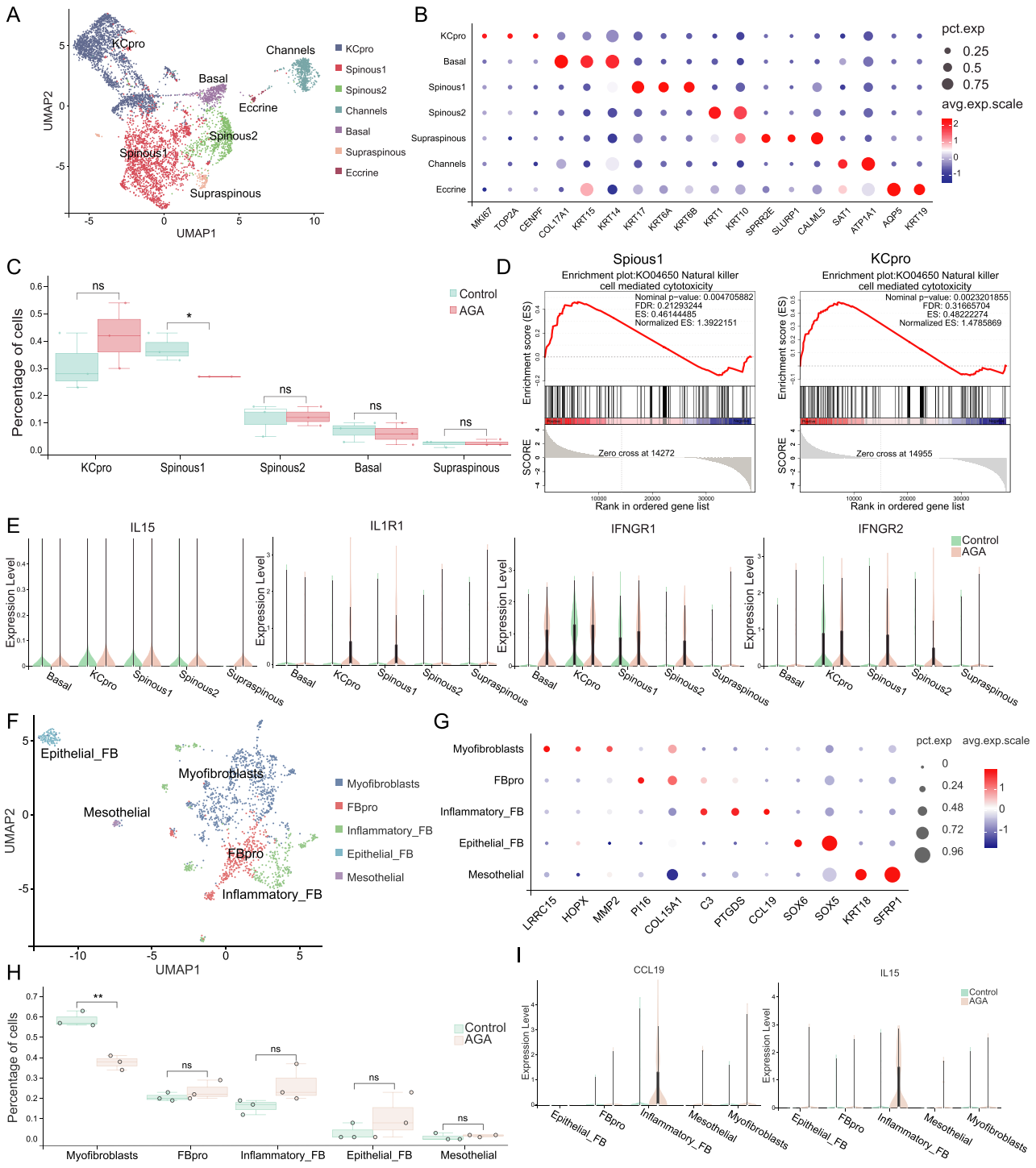

Figure 6 Heterogeneity of fibroblasts and keratinocytes from the hair follicle snRNA-seq dataset. (**A, F**) UMAP plots depicting the clusters of keratinocytes and fibroblasts identified in hair follicles. (**B, G**) Dot plots showing the markers characteristic of the respective keratinocyte and fibroblast subsets. (**C, H**) Percentage distribution of keratinocyte or fibroblast subset within the total cell population (*$p < 0.05$, **$p < 0.01$). (**D**) GSEA plot of the natural killer cell-mediated cytotoxicity pathway in Spinous1 and KCpro subset. (**E, I**) Violin plots illustrating the expression of genes associated with NK and CD8+ T cells.
Abbreviations: KC, Keratinocyte; FB, Fibroblast; pro, proliferating.

across the groups, while a significant decrease in spinous1 KCs was observed in balding hair follicles (Figure 6C and Supplementary Data 3). GSEA revealed significant enrichment of natural killer cell mediated cytotoxicity pathways in the KCpro and spinous1 KCs of balding hair follicle (Figure 6D). *IL15, IL33, IL1R1*, and interferon gamma receptors 1

and 2 (*IFNGR1* and *IFNGR2*), which associated with cytotoxic of NK and CD8+ T cells, were also found to be upregulated in the KCs of balding hair follicles (Figure 6E).

Fibroblasts (FBs) play a vital role in hair growth by producing and maintaining the connective tissue that supports the hair follicle's function. In our study, we examined the heterogeneity of FBs in patients with AGA and identified five distinct subgroups through secondary analysis (Figure 6F and G). The largest subgroup was myofibroblasts, characterized by the markers *LRRC15*$^+$*HOPX*$^+$*MMP2*$^+$. Other identified subgroups included proliferating fibroblasts (FBpro), marked by *COL15A1*$^+$*PI16*$^+$; epithelial FBs (*SOX5*$^+$*SOX6*$^+$); mesothelial FBs (*KRT18*$^+$*SFRP1*$^+$); and inflammatory FBs (*C3*$^+$*CCL19*$^+$PTGDS$^+$) (Figure 6F and G, Supplementary Data 2). In balding hair follicles, the number of myofibroblasts was significantly reduced. While no significant differences were observed in the inflammatory FBs, there was a noticeable upward trend in their numbers within balding hair follicles (Figure 6H, Supplementary Data 3). Additionally, the expression of CCL19, a cytokine secreted by fibroblasts that enhances the recruitment of CD8$^+$ T and NK cells,[38–40] was elevated in the inflammatory FBs of balding hair follicles. Similarly, IL-15 expression was also upregulated in inflammatory FBs (Figure 6I).

Discussion

It is well-established that microinflammation and abnormal immune responses occur in the hair follicles of AGA, yet the exact patterns of immune dysregulation remain unclear. Our bulk RNA-seq analysis showed that inflammation in grade 5 AGA patients' balding hair follicles is significantly more severe than in those with grades 3 and 4. snRNA-seq further revealed notable differences in the proportions of NK and CD8$^+$ T cells between balding and non-balding follicles. GSEA showed significant enrichment of NK cell-mediated cytotoxicity and cytokine-receptor interaction pathways in the balding group. IL-15 promotes the expansion and maintenance of CD8$^+$ T cells and NK cells while enhancing the production of granzymes, IFN-γ, and TNF-α by CD8+ T cells and NK cells, thereby strengthening cytotoxic and inflammatory responses;[41–43] our results further show that IL-15 is highly expressed in BECs, keratinocytes, and fibroblasts, suggesting that CD8$^+$ T and NK cells may inhibit hair follicle regeneration via IL-15-mediated crosstalk with these structural cells.

Although AGA is traditionally considered a non-inflammatory, non-scarring form of alopecia, histological analysis shows evidence of inflammation. One study found that moderate inflammatory infiltrates and fibrosis were present in 36.8% of AGA patients, significantly higher than the 9.1% observed in control subjects.[44] Our research show that early inflammatory responses in AGA are relatively mild, which may the reason of its classification as a non-inflammatory form of hair loss. However, as AGA progresses, inflammation becomes more pronounced, and the impact of immune responses on hair loss becomes increasingly significant. Therefore, we focused on research later-stage AGA patients classified as grade 5 hair loss according to the Hamilton–Norwood system.

Research on immune cell regulation in AGA is still in its early stages, and there is currently limited understanding of the specific role immune cells play in AGA. To date, previous study has reported that the increase in γδ T cells, central memory CD8$^+$ T cells, activated CD8$^+$ T cells and mast cell infiltration contributes to changes in the immune microenvironment in male AGA.[10] Charoensuksira et al used the scalps of normal patients as controls and found an enrichment of CD4$^+$ helper T cells in AGA patients.[45] In our study, we selected the occipital area of AGA patients as the control group, based on the observation that this region is less susceptible to androgenetic alopecia-related hair loss. We observed significant differences in the proportions of NK and CD8$^+$ T cells between balding and non-balding. Comparing the frontal balding area with occipital normal areas can provide difference insights into the molecular mechanisms underlying the condition. CD8$^+$ T cells have been shown to play a role in immune-mediated alopecia like alopecia areata,[46] primary cicatricial alopecia,[47] and frontal fibrosing alopecia.[48] Moreover, IFN-γ and various other cytokines are pivotal players in alopecia. Our result show that IFN-γ, TNFα, and cytotoxic granules, including PRF1, GZMA and GZMB increased in balding hair follicle of grade 5 AGA patients. These findings suggest that immune-mediated mechanisms, including specific T cell populations and inflammatory cytokines, may play a critical role in the pathogenesis of AGA.

Insufficient perifollicular vascularization contributes to premature functional senescence of hair follicles, thereby impeding the transition from telogen to anagen phase in the hair cycle.[49] Our findings demonstrating reduced expression of angiogenesis-associated genes (VEGFC, VWF, FGFR1/2) in balding hair follicle parallel previous reports that DHT-mediated suppression of angiogenic pathways diminishes perifollicular capillary density,[50] a critical pathomechanism in androgen-related alopecia. The therapeutic implications of vascular regeneration strategies are further corroborated by existing evidence: Platelet-rich plasma

promotes hair follicle regrowth through Wnt/β-catenin reactivation,[51] while minoxidil's vasodilatory effects via potassium channel activation in dermal vasculature[52] and transdermal therapeutic platforms utilizing VEGF/Ritlecitinib-encapsulated polyhydroxyalkanoate nanoparticles demonstrate efficacy in AGA treatment. The dual-action mechanism combines Ritlecitinib's selective JAK3/TEC kinase inhibition - suppressing pathogenic $CD8^+$ T cell and natural killer (NK) cell activity - with VEGF's pro-angiogenic signaling, synergistically promoting hair follicular regeneration.[2] These therapeutic outcomes align with our molecular findings of upregulated IL15 and RORA in balding follicle BECs, suggesting compensatory vascular niche remodeling that may functionally interface with the dual immunovascular regulatory axis. Specifically, NK cells and $CD8^+$ T lymphocytes exhibit context-dependent angiocrine modulation through IL15-mediated cytokine cascades and paracrine VEGF signaling pathways in androgen-driven alopecia pathogenesis.

Keratin is a cytoskeletal protein that forms intermediate filaments in epithelial cells, playing a key role in maintaining their structural integrity. It is also a major component of hair, where it contributes significantly to its mechanical strength.[53] In response to skin injury, keratinocytes (KCs) located near the wound site upregulate the expression of *KRT16, KRT17*, and *KRT6*, signaling a highly activated and proliferative state.[54] Interestingly, we observed that spinous1 KCs, which exhibit high levels of *KRT16, KRT17* and *KRT6*, show a significant reduction in bald hair follicles. However, the exact relationship between hair growth and spinous1 KCs remains to be fully elucidated and warrants further investigation.

Limitation

This study has several limitations that should be considered. First, while snRNA-seq is capable of identifying a broader and more comprehensive range of cell types, it has a key limitation in that it excludes RNA molecules from the cytoplasm. This means it may not capture the full spectrum of cellular transcriptional states. Second, the variability observed in findings related to inflammatory infiltration in AGA can be influenced by several factors, including the age of the participants, the severity of their condition, and the different methodologies used to assess and quantify inflammation. Finally, the statistical power of our AGA study is constrained by limited sample size and substantial interindividual heterogeneity, potentially compromising result generalizability. Notably, the observed directional trends in selected gene expression profiles (Figure 4A) lacked statistical significance. These methodological limitations underscore the necessity for expanded human subject recruitment in subsequent validation studies.

Conclusion

This study combines bulk and single-nucleus RNA sequencing to characterize the immune microenvironment of AGA hair follicles, revealing NK and CD8+ T cells are hyperactivated in disease progression. The overexpression of IL-15 in BECs suggests that IL-15-mediated immune activation and vascular compromise synergistically drive AGA pathogenesis. Future studies should employ single-cell multi-omics to resolve $CD8^+$ subset dynamics, validate IL-15/JAK inhibition in 3D organoid models, and map spatial crosstalk between semaphorin-guided immune trafficking and pericyte dysfunction.

Resource Availability

The raw snRNA-seq and bulk RNA-seq data in this paper format generated in this study have been submitted to the Genome Sequence Archive (GSA) database under the accession codes HRA007210 and HRA009430 (https://ngdc.cncb.ac.cn/gsa-human). All other data can be found in the article and its Supplementary files. For additional information or requests for reagents and resources, please contact the lead investigator, Shijun Shan, at shanshijun2023@163.com.

Institutional Review Board Statement

This study was approved by the Human Research Ethics Committee of Xiang'an Hospital of Xiamen University (XAHLL2023011).

Acknowledgments

This work is supported by the Natural Science Foundation Committee of China (Grant No.81972953), Fund for Less Developed Regions of the National Natural Science Foundation of China (Grant No. 82160601) and Guizhou Provincial Science and Technology Projects, ZK [2022] general 250.

Disclosure

The authors declare no conflicts of interest in this work.

References

1. Pirastu N, Joshi PK, de Vries PS, et al. GWAS for male-pattern baldness identifies 71 susceptibility loci explaining 38% of the risk. *Nat Commun*. 2017;8(1):1584. doi:10.1038/s41467-017-01490-8
2. Ding YW, Li Y, Zhang ZW, et al. Hydrogel forming microneedles loaded with VEGF and Ritlecitinib/polyhydroxyalkanoates nanoparticles for mini-invasive androgenetic alopecia treatment. *Bioact Mater*. 2024;38:95–108. doi:10.1016/j.bioactmat.2024.04.020
3. Yap CX, Sidorenko J, Wu Y, et al. Dissection of genetic variation and evidence for pleiotropy in male pattern baldness. *Nat Commun*. 2018;9(1):5407. doi:10.1038/s41467-018-07862-y
4. Heilmann-Heimbach S, Herold C, Hochfeld LM, et al. Meta-analysis identifies novel risk loci and yields systematic insights into the biology of male-pattern baldness. *Nat Commun*. 2017;8:14694. doi:10.1038/ncomms14694
5. Yuan A, Xia F, Bian Q, et al. Ceria nanozyme-integrated microneedles reshape the perifollicular microenvironment for androgenetic alopecia treatment. *ACS Nano*. 2021;15(8):13759–13769. doi:10.1021/acsnano.1c05272
6. Haslam IS, Jadkauskaite L, Szabó IL, et al. Oxidative damage control in a human (Mini-) organ: nrf2 activation protects against oxidative stress-induced hair growth inhibition. *J Invest Dermatol*. 2017;137(2):295–304. doi:10.1016/j.jid.2016.08.035
7. Heymann WR. The inflammatory component of androgenetic alopecia. *J Am Acad Dermatol*. 2022;86(2):301–302. doi:10.1016/j.jaad.2021.11.013
8. Mahé YF, Michelet JF, Billoni N, et al. Androgenetic alopecia and microinflammation. *Int J Dermatol*. 2000;39(8):576–584. doi:10.1046/j.1365-4362.2000.00612.x
9. Merlotto MR, Ramos PM, Miot HA. Pattern hair loss: assessment of microinflammation in miniaturized and terminal hair follicles through horizontal histologic sections. *J Am Acad Dermatol*. 2020;83(2):e145–e46. doi:10.1016/j.jaad.2020.03.119
10. Xiong HD, Tang LL, Chen HJ, et al. Identification of immune microenvironment changes, immune-related pathways and genes in male androgenetic alopecia. *Medicine*. 2023;102(38):e35242. doi:10.1097/MD.0000000000035242
11. Jaworsky C, Kligman AM, Murphy GF. Characterization of inflammatory infiltrates in male pattern alopecia: implications for pathogenesis. *Br J Dermatol*. 1992;127(3):239–246. doi:10.1111/j.1365-2133.1992.tb00121.x
12. Rahmani W, Sinha S, Biernaskie J. Immune modulation of hair follicle regeneration. *NPJ Regen Med*. 2020;5:9. doi:10.1038/s41536-020-0095-2
13. Takahashi R, Grzenda A, Allison TF, et al. Defining transcriptional signatures of human hair follicle cell states. *J Invest Dermatol*. 2020;140(4):764–73.e4. doi:10.1016/j.jid.2019.07.726
14. Butler A, Hoffman P, Smibert P, et al. Integrating single-cell transcriptomic data across different conditions, technologies, and species. *Nat Biotechnol*. 2018;36(5):411–420. doi:10.1038/nbt.4096
15. Korsunsky I, Millard N, Fan J, et al. Fast, sensitive and accurate integration of single-cell data with Harmony. *Nat Methods*. 2019;16(12):1289–1296. doi:10.1038/s41592-019-0619-0
16. Kobak D, Berens P. The art of using t-SNE for single-cell transcriptomics. *Nat Commun*. 2019;10(1):5416. doi:10.1038/s41467-019-13056-x
17. Kanehisa M, Furumichi M, Sato Y, et al. KEGG for taxonomy-based analysis of pathways and genomes. *Nucleic Acids Res*. 2023;51(D1):D587–d92. doi:10.1093/nar/gkac963
18. Wu S, Yu Y, Liu C, et al. Single-cell transcriptomics reveals lineage trajectory of human scalp hair follicle and informs mechanisms of hair graying. *Cell Discov*. 2022;8(1):49. doi:10.1038/s41421-022-00394-2
19. Jensen KB, Collins CA, Nascimento E, et al. Lrig1 expression defines a distinct multipotent stem cell population in mammalian epidermis. *Cell Stem Cell*. 2009;4(5):427–439. doi:10.1016/j.stem.2009.04.014
20. Kadaja M, Keyes BE, Lin M, et al. SOX9: a stem cell transcriptional regulator of secreted niche signaling factors. *Genes Dev*. 2014;28(4):328–341. doi:10.1101/gad.233247.113
21. Lee J, Rabbani CC, Gao H, et al. Hair-bearing human skin generated entirely from pluripotent stem cells. *Nature*. 2020;582(7812):399–404. doi:10.1038/s41586-020-2352-3
22. Schmidt M, Hansmann F, Loeffler-Wirth H, et al. A spatial portrait of the human sebaceous gland transcriptional program. *J Biol Chem*. 2024;300(7):107442. doi:10.1016/j.jbc.2024.107442
23. Downie MM, Sanders DA, Maier LM, et al. Peroxisome proliferator-activated receptor and farnesoid X receptor ligands differentially regulate sebaceous differentiation in human sebaceous gland organ cultures in vitro. *Br J Dermatol*. 2004;151(4):766–775. doi:10.1111/j.1365-2133.2004.06171.x
24. Dobson H, Tilston V, Ressel L. Immunolocalization of c-Fos, ELOVL5 and oestradiol in the ewe vulva in relation to oestrus behaviour after treatment with lipopolysaccharide. *Reprod Domest Anim*. 2020;55(2):137–145. doi:10.1111/rda.13594
25. Williams DW, Greenwell-Wild T, Brenchley L, et al. Human oral mucosa cell atlas reveals a stromal-neutrophil axis regulating tissue immunity. *Cell*. 2021;184(15):4090–104.e15. doi:10.1016/j.cell.2021.05.013
26. Ober-Reynolds B, Wang C, Ko JM, et al. Integrated single-cell chromatin and transcriptomic analyses of human scalp identify gene-regulatory programs and critical cell types for hair and skin diseases. *Nat Genet*. 2023;55(8):1288–1300. doi:10.1038/s41588-023-01445-4
27. Bangert C, Alkon N, Chennareddy S, et al. Dupilumab-associated head and neck dermatitis shows a pronounced type 22 immune signature mediated by oligoclonally expanded T cells. *Nat Commun*. 2024;15(1):2839. doi:10.1038/s41467-024-46540-0
28. Long H, Espinosa L, Sawalha AH. Unraveling the immunomodulatory impact of hydroxychloroquine on peripheral T cells using single-cell RNA sequencing. *J Autoimmun*. 2024;149:103324. doi:10.1016/j.jaut.2024.103324
29. Zhang Y, Bai Y, Ma XX, et al. Clinical-mediated discovery of pyroptosis in CD8(+) T cell and NK cell reveals melanoma heterogeneity by single-cell and bulk sequence. *Cell Death Dis*. 2023;14(8):553. doi:10.1038/s41419-023-06068-5
30. Cheng Y, Sun F, Alapat DV, et al. Multi-omics reveal immune microenvironment alterations in multiple myeloma and its precursor stages. *Blood Cancer J*. 2024;14(1):194. doi:10.1038/s41408-024-01172-x
31. Casneuf T, Adams HC, van de Donk N, et al. Deep immune profiling of patients treated with lenalidomide and dexamethasone with or without daratumumab. *Leukemia*. 2021;35(2):573–584. doi:10.1038/s41375-020-0855-4

32. Santana-Hernández S, Suarez-Olmos J, Servitja S, et al. NK cell-triggered CCL5/IFNγ-CXCL9/10 axis underlies the clinical efficacy of neoadjuvant anti-HER2 antibodies in breast cancer. *J Exp Clin Cancer Res*. 2024;43(1):10. doi:10.1186/s13046-023-02918-4
33. Luda KM, Longo J, Kitchen-Goosen SM, et al. Ketolysis drives CD8(+) T cell effector function through effects on histone acetylation. *Immunity*. 2023;56(9):2021–35.e8. doi:10.1016/j.immuni.2023.07.002
34. Van Den Eeckhout B, Ballegeer M, De Clercq J, et al. Rethinking IL-1 antagonism in respiratory viral infections: a role for IL-1 signaling in the development of antiviral T cell immunity. *Int J Mol Sci*. 2023;24(21):15770. doi:10.3390/ijms242115770
35. Arrizabalaga L, Risson A, Ezcurra-Hualde M, et al. Unveiling the multifaceted antitumor effects of interleukin 33. *Front Immunol*. 2024;15:1425282. doi:10.3389/fimmu.2024.1425282
36. Burkett PR, Koka R, Chien M, et al. Coordinate expression and trans presentation of interleukin (IL)-15Ralpha and IL-15 supports natural killer cell and memory CD8+ T cell homeostasis. *J Exp Med*. 2004;200(7):825–834. doi:10.1084/jem.20041389
37. Ma F, Plazyo O, Billi AC, et al. Single cell and spatial sequencing define processes by which keratinocytes and fibroblasts amplify inflammatory responses in psoriasis. *Nat Commun*. 2023;14(1):3455. doi:10.1038/s41467-023-39020-4
38. Kersh AE, Sati S, Huang J, et al. CXCL9, CXCL10, and CCL19 synergistically recruit T lymphocytes to skin in lichen planus. *JCI Insight*. 2024;9(20). doi:10.1172/jci.insight.179899
39. Zhang Y, Liu G, Zeng Q, et al. CCL19-producing fibroblasts promote tertiary lymphoid structure formation enhancing anti-tumor IgG response in colorectal cancer liver metastasis. *Cancer Cell*. 2024;42(8):1370–85.e9. doi:10.1016/j.ccell.2024.07.006
40. Zhou Z, Li J, Hong J, et al. Interleukin-15 and chemokine ligand 19 enhance cytotoxic effects of chimeric antigen receptor T cells using zebrafish xenograft model of gastric cancer. *Front Immunol*. 2022;13:1002361. doi:10.3389/fimmu.2022.1002361
41. Hangasky JA, Fernández RDV, Stellas D, et al. Leveraging long-acting IL-15 agonists for intratumoral delivery and enhanced antimetastatic activity. *Front Immunol*. 2024;15:1458145. doi:10.3389/fimmu.2024.1458145
42. Lensing M, Jabbari A. An overview of JAK/STAT pathways and JAK inhibition in alopecia areata. *Front Immunol*. 2022;13:955035. doi:10.3389/fimmu.2022.955035
43. Mishra A, Sullivan L, Caligiuri MA. Molecular pathways: interleukin-15 signaling in health and in cancer. *Clin Cancer Res*. 2014;20(8):2044–2050. doi:10.1158/1078-0432.CCR-12-3603
44. Whiting DA. Chronic telogen effluvium: increased scalp hair shedding in middle-aged women. *J Am Acad Dermatol*. 1996;35(6):899–906. doi:10.1016/S0190-9622(96)90113-9
45. Charoensuksira S, Tantiwong S, Pongklaokam J, et al. Disturbance of immune microenvironment in androgenetic alopecia through spatial transcriptomics. *Int J Mol Sci*. 2024;25(16):9031. doi:10.3390/ijms25169031
46. King BA, Craiglow BG. Janus kinase inhibitors for alopecia areata. *J Am Acad Dermatol*. 2023;89(2s):S29–s32. doi:10.1016/j.jaad.2023.05.049
47. Ezemma O, Devjani S, Kelley KJ, et al. Treatment modalities for lymphocytic and neutrophilic scarring alopecia. *J Am Acad Dermatol*. 2023;89(2s):S33–s35. doi:10.1016/j.jaad.2023.04.023
48. Costa Fechine CO, Sakai Valente NY, Romiti R, et al. Correlation of clinical and trichoscopy features with the degree of histologic inflammation in lichen planopilaris and frontal fibrosing alopecia in a cross-sectional study. *J Am Acad Dermatol*. 2024;91(1):161–163. doi:10.1016/j.jaad.2024.03.017
49. Chen Y, Ren T, Wu W, et al. Gas-propelled anti-hair follicle aging microneedle patch for the treatment of androgenetic alopecia. *J Control Release*. 2025;379:636–651. doi:10.1016/j.jconrel.2025.01.034
50. Anjum MA, Zulfiqar S, Chaudhary AA, et al. Stimulation of hair regrowth in an animal model of androgenic alopecia using 2-deoxy-D-ribose. *Front Pharmacol*. 2024;15:1370833. doi:10.3389/fphar.2024.1370833
51. Abdin R, Zhang Y, Jimenez JJ. Treatment of androgenetic alopecia using PRP to target dysregulated mechanisms and pathways. *Front Med*. 2022;9:843127. doi:10.3389/fmed.2022.843127
52. Olsen EA, Sinclair R, Hordinsky M, et al. Summation and recommendations for the safe and effective use of topical and oral minoxidil. *J Am Acad Dermatol*. 2025. doi:10.1016/j.jaad.2025.04.016
53. An SY, Kim HS, Kim SY, et al. Keratin-mediated hair growth and its underlying biological mechanism. *Commun Biol*. 2022;5(1):1270. doi:10.1038/s42003-022-04232-9
54. Zhang X, Yin M, Zhang LJ. Keratin 6, 16 and 17-critical barrier alarmin molecules in skin wounds and psoriasis. *Cells*. 2019;8(8):807. doi:10.3390/cells8080807